

Structural and magnetic studies of Fe-implanted α -Al₂O₃

E. Alves^{a,b,*}, C. MacHargue^c, R.C. Silva^{a,b}, C. Jesus^{a,b}, O. Conde^d,
M.F. da Silva^{a,b}, J.C. Soares^{a,b}

^aInstituto Tecnológico e Nuclear, Department of Physics, EN 10, 2686-953 Sacavém, Portugal

^bCFNUL, Av. Prof. Gama Pinto 2, 1699 Lisbon, Portugal

^cCenter for Materials Processing, University of Tennessee, Knoxville, TN 37996-2350, USA

^dDepartment of Physics-FCUL, Ed. C1, Campo Grande, 1700 Lisbon, Portugal

Abstract

High fluence implantation of Fe in α -Al₂O₃ and post-implantation annealing leads to the formation of various phases in the near-surface region whose nature depend upon the annealing atmosphere and crystal orientation. The structural evolution of the near-surface region and the magnetic properties of samples oriented with either the *c*-axis or *a*-axis normal to the surface and annealed in oxidizing and reducing atmospheres were studied with glancing incidence X-ray diffraction (GIXRD), transmission electron microscopy (TEM), Rutherford backscattering (RBS)/channelling and vibrating sample magnetometry (VSM). The as-implanted samples contained metallic iron clusters in a damaged matrix. This matrix became amorphous for fluences of 2×10^{17} Fe⁺/cm² and above. The annealing in oxidizing atmosphere of the samples with the *a*-axis normal to the surface leads to the formation of a mixed layer containing α -Al₂O₃ and Fe₂O₃. The magnetization measurements indicate the presence of a large superparamagnetic contribution and a small ferromagnetic component. Annealing in a reducing atmosphere promotes the in-diffusion of iron and the magnetization decreases. A similar annealing of the sample with *c*-axis normal to the surface induces coalescence of precipitates in a discontinuous buried film of metallic iron parallel to the *c*-plane with a strong ferromagnetic signal and a small superparamagnetic contribution. The magnetization increases with the annealing temperature. © 2000 Elsevier Science S.A. All rights reserved.

Keywords: Fe precipitates; Magnetization; Sapphire; Orientation dependence

1. Introduction

The formation of buried magnetic layers in oxides allows the development of very attractive structures for magnetic recording technologies [1]. Due to its high chemical and mechanical stability, sapphire (α -Al₂O₃) is one of the most important oxides for such applications. The production of magnetic buried layers can be achieved through the implantation of high fluences of magnetic ions. By choosing beam energy and ion flu-

ence it is possible to control the depth and thickness of the magnetic layers. Indeed, MacHargue et al. observed the formation of elongated platelets in high fluence iron-implanted sapphire [2], the dimensions and distribution of which depend on the implantation conditions (e.g. energy and ion fluence). They noticed also that the final state of the system was influenced by the annealing conditions [3,4]. In all this work no evidence was found for any effect of the substrate orientation on the iron behaviour. Furthermore, although some studies on the magnetic properties of iron implanted sapphire have been done [5,6], the influence of substrate orientation, annealing conditions and ion fluence on these properties was not investigated to date.

In this study we report on the magnetic and struc-

* Corresponding author. Tel: +351-1-9946086; fax: +351-1-9941525.

E-mail address: ealves@itn1.itn.pt (E. Alves).

tural behaviour of iron implanted *a*- and *c*-cut α - Al_2O_3 . Samples implanted with different fluences were annealed in oxidizing and reducing atmospheres. The structural changes were followed by glancing incidence X-ray diffraction (GIXRD), transmission electron microscopy (TEM) and Rutherford backscattering spectrometry (RBS), while a vibrating sample magnetometer (VSM) was used to measure the magnetic behaviour. In this way, we could follow in detail the relationship between the microstructural evolution and magnetic properties.

2. Experimental

High purity α - Al_2O_3 single crystals with optically polished surfaces cut perpendicularly to the $\langle 0001 \rangle$ axis (*c*-samples) and $\langle 11\bar{2}0 \rangle$ axis (*a*-samples) were implanted with 160 keV Fe^+ ions to fluences in the range of 1×10^{17} to 4×10^{17} at./ cm^2 . The samples were tilted 7° with respect to the ion beam to avoid channelling and held at room temperature. The range of the implanted ions was 72 nm. Thermal annealings were carried out at 700°C , 800°C and 1100°C for 1 h in reducing (4% hydrogen–argon mixture) and oxidizing atmospheres.

RBS/channeling studies were performed with a 1.6 and 2 MeV He^+ beam after implantation and after

each stage of thermal annealing. The backscattered particles were detected at 160° and close to 180° using silicon surface barrier detectors with resolutions of 13 and 18 keV, respectively. In order to minimize the effects of charge accumulation on the Al_2O_3 surface during analysis, the crystal was masked with a thin Ni foil with a 4-mm hole. A Siemens D-5000 spectrometer, allowing both conventional (Bragg–Brentano) and grazing incidence geometries, was used to perform the X-ray diffraction studies. The diffraction patterns were recorded using the Cu $\text{K}\alpha$ radiation at 0.5° angle of incidence to the specimen surface. The identification of crystalline phases was done using the JCPDS database cards [7]. Transmission electron microscopy observations were done with a Hitachi HF-2000 field emission electron microscope operating at 200 kV. The magnetization curves were obtained with a Digital Measurement System magnetometer, model DMS 880.

3. Results

3.1. (0001) α - Al_2O_3

The RBS spectra of Fig. 1 shows the annealing behaviour under reducing conditions of two samples implanted with 1×10^{17} Fe^+/cm^2 and 2×10^{17} Fe^+/cm^2 . We can see that no significant change occurs

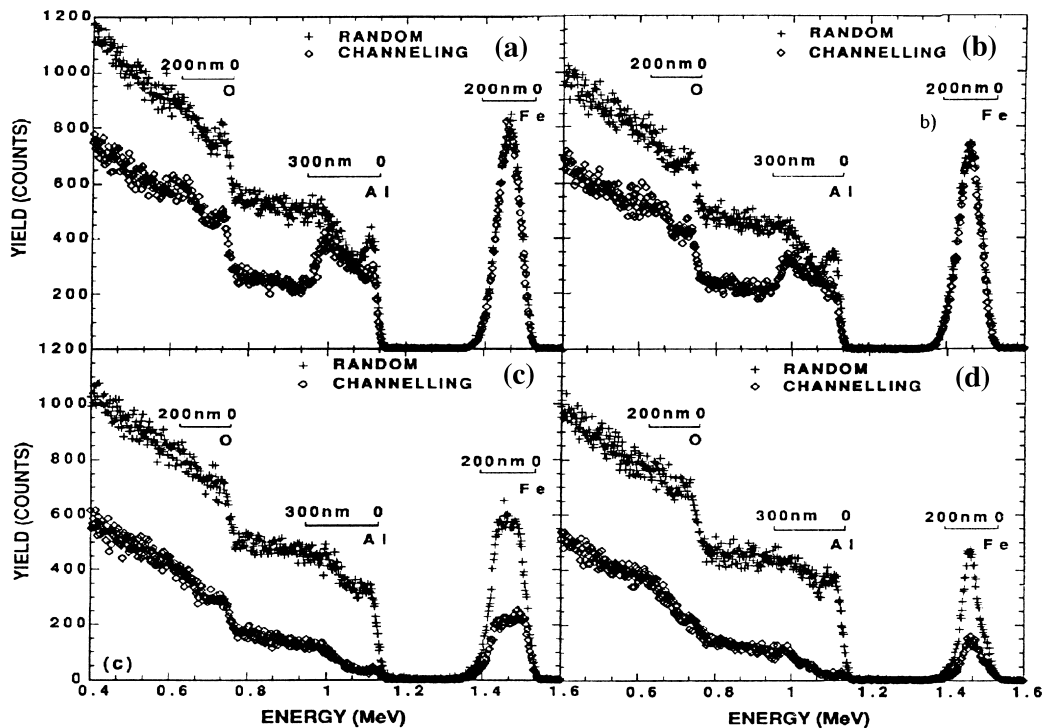


Fig. 1. Aligned and random RBS spectra of *c*-axis-oriented sapphire implanted with 2×10^{17} Fe^+/cm^2 before (a) and after the annealing at 700°C (b) and 1100°C (c) in a reducing atmosphere. The results of a sample implanted with 1×10^{17} Fe^+/cm^2 were also shown in (d) for comparison.

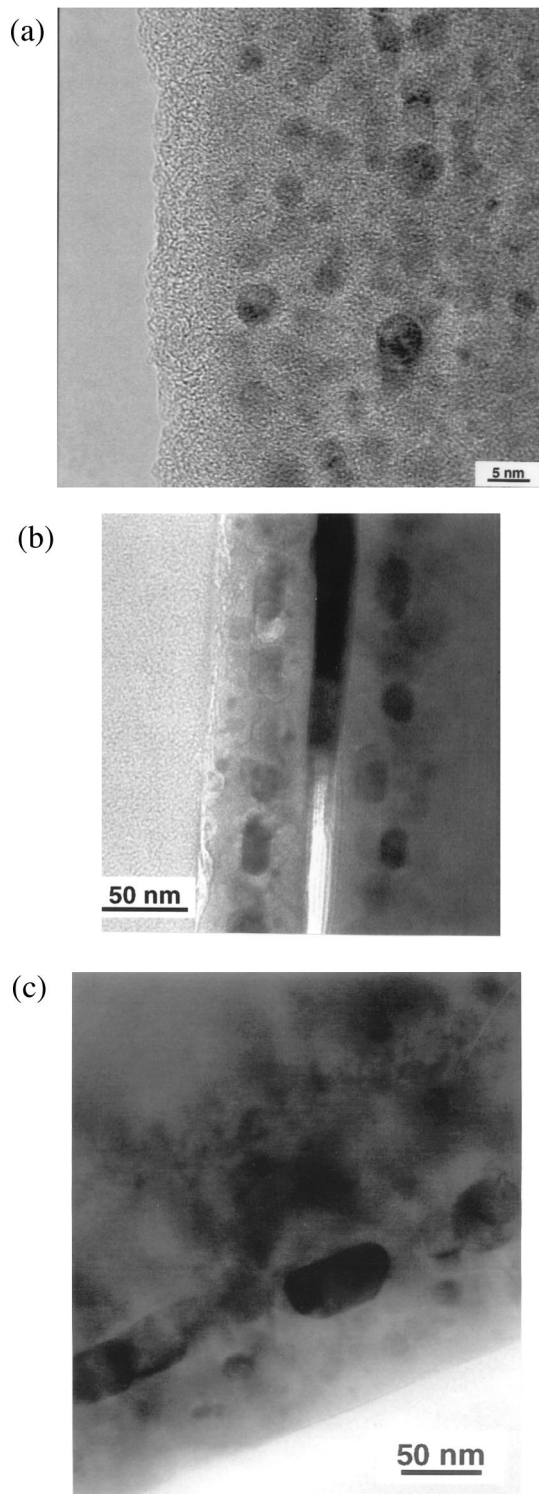


Fig. 2. Micrographs of the as-implanted (a) and annealed at 1100°C (b) in reducing atmosphere of *c*-axis-oriented samples implanted with $2 \times 10^{17} \text{ Fe}^+/\text{cm}^2$. The micrograph of a sample implanted with $1 \times 10^{17} \text{ Fe}^+/\text{cm}^2$ and submitted to the same annealing is shown in (c).

up to 700°C. The annealing at 1100°C produces a great reduction of the implantation damage, visible through the decrease of the yield on the sapphire aligned spec-

trum. However, the as-implanted Gaussian profile of iron became rectangular and the maximum peak concentration decreased but no loss of iron was detected. The reduction observed in the iron yield in the aligned spectrum reveals that approximately 50% of the ions were incorporated at substitutional lattice sites or interstitial sites shadowed by the matrix atoms along this direction. These changes are compatible with the formation of iron precipitates coherently aligned with the $\langle 0001 \rangle$ axis of $\alpha\text{-Al}_2\text{O}_3$.

The presence of the precipitates is revealed in the micrographs of the cross-sectioned samples of Fig. 2. Precipitates with diameters in the range of 5–20 nm were found in samples implanted with $2 \times 10^{17} \text{ Fe}^+/\text{cm}^2$ even after implantation (Fig. 2a). This is in agreement with previous studies by Ren et al. who showed that the precipitates consist mainly of crystalline body-centred cubic $\alpha\text{-Fe}$ [8]. The annealing induces the coalescence of the precipitates leading to the formation of two distinct regions. At the front and rear edges of the iron profile we see a disperse distribution of small precipitates. Large precipitates with a rectangular shape were found at a depth close to the range where the maximum Fe concentration was located forming a discontinuous band parallel to the surface. The length of the precipitates increases with the fluence of the implanted ions. The formation of such precipitates suggests that iron diffuse faster parallel to the *c*-plane.

Fig. 3 shows the influence of the annealing temperature on the magnetic behaviour of the sapphire sample implanted with $2 \times 10^{17} \text{ Fe}^+/\text{cm}^2$. For comparison we show the result obtained for a sample implanted with $1 \times 10^{17} \text{ Fe}^+/\text{cm}^2$ after annealing at 1100°C, since at lower temperatures only the diamagnetic contribution of sapphire is seen. After implantation the curve of the sample implanted with $2 \times 10^{17} \text{ Fe}^+/\text{cm}^2$ shows the presence of a diamagnetic contribution of the sapphire and the presence of a small ferromagnetic signal responsible for the hysteresis of the curve. The magnetization increases with the annealing temperature, with the ferromagnetic contribution being dominant with a small superparamagnetic signal, which causes the ‘S’ shape of the curve. The increase of the magnetization with the annealing temperature and the dose is clearly correlated with the growing of the precipitates due to the coalescence mechanism.

3.2. $(11\bar{2}0)$ $\alpha\text{-Al}_2\text{O}_3$

Fig. 4 compares the annealing behaviour of sapphire implanted with $1 \times 10^{17} \text{ Fe}^+/\text{cm}^2$ and $4 \times 10^{17} \text{ Fe}^+/\text{cm}^2$ annealed in reducing and oxidizing atmospheres. For the samples implanted with the lower dose iron starts to diffuse to the surface during the annealing at 800°C in both annealing conditions (not shown).

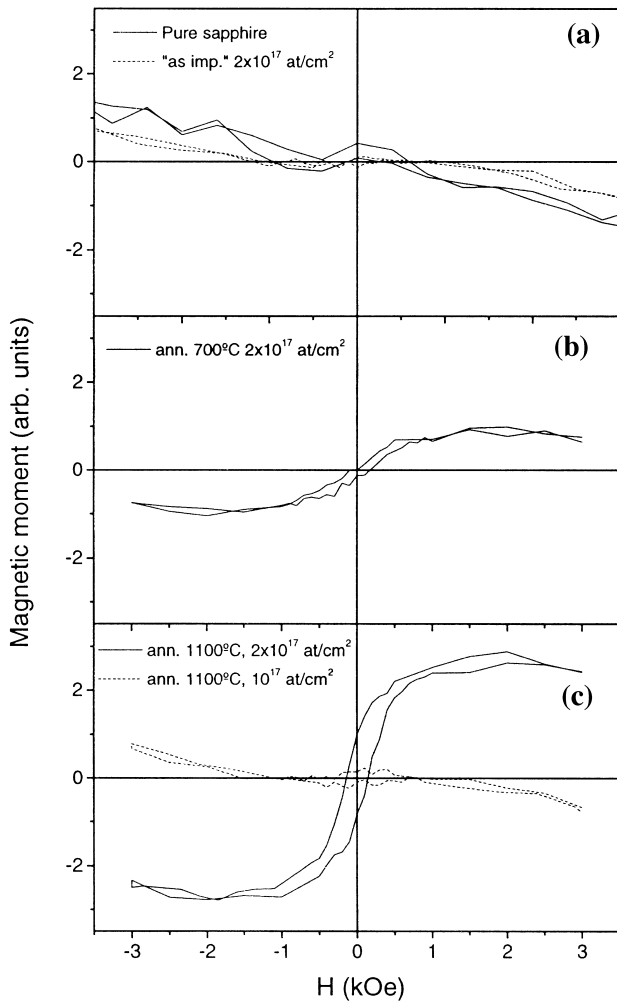


Fig. 3. Magnetization curves for the virgin and as-implanted *c*-axis-oriented sapphire with $2 \times 10^{17} \text{ Fe}^+/\text{cm}^2$ (a) and after annealing at 700°C (b) and 1100°C (c) in reducing atmosphere. The dashed curve in (c) was obtained for a sample implanted with $1 \times 10^{17} \text{ Fe}^+/\text{cm}^2$.

The amount of iron at the surface for the sample annealed in an oxidizing atmosphere increased with the annealing temperature (Fig. 4b); while for the samples annealed in reducing atmosphere a large redistribution of iron occurred and approximately 60% of the Fe was lost (Fig. 4c). Under oxidizing conditions the presence of free oxygen allows the formation of iron oxides at the surface and may explain this different behaviour. The changes in the Fe profile agree with the assumption made above that the diffusion along the *c*-plane is much easier (notice that in these samples the *c*-plane is perpendicular to the surface). The damage recovery is also different as is evident from the large difference in the minimum yields along the $\langle 11\bar{2}0 \rangle$ axis of the samples annealed in the oxidizing (35%) and reducing atmospheres (3%). Combining these results with those found for the *c*-samples we conclude that the microstructure developed in the implanted region inhibits

the damage recovery as was also observed in other works [9]. The presence of Fe_2O_3 in the samples annealed in oxidizing atmosphere was confirmed by GIXRD. Fig. 5 shows the X-ray spectra of the samples implanted with $4 \times 10^{17} \text{ Fe}^+/\text{cm}^2$ after implantation and after annealing at 1100°C in an oxidizing atmosphere, respectively. The presence of metallic iron precipitates in the samples was observed immediately after implantation in agreement with TEM observations. The annealing in oxidizing atmosphere induces the formation of hematite (Fe_2O_3), as shown by the X-ray diffraction spectrum. This transformation was also noticed by the change in coloration from metallic to

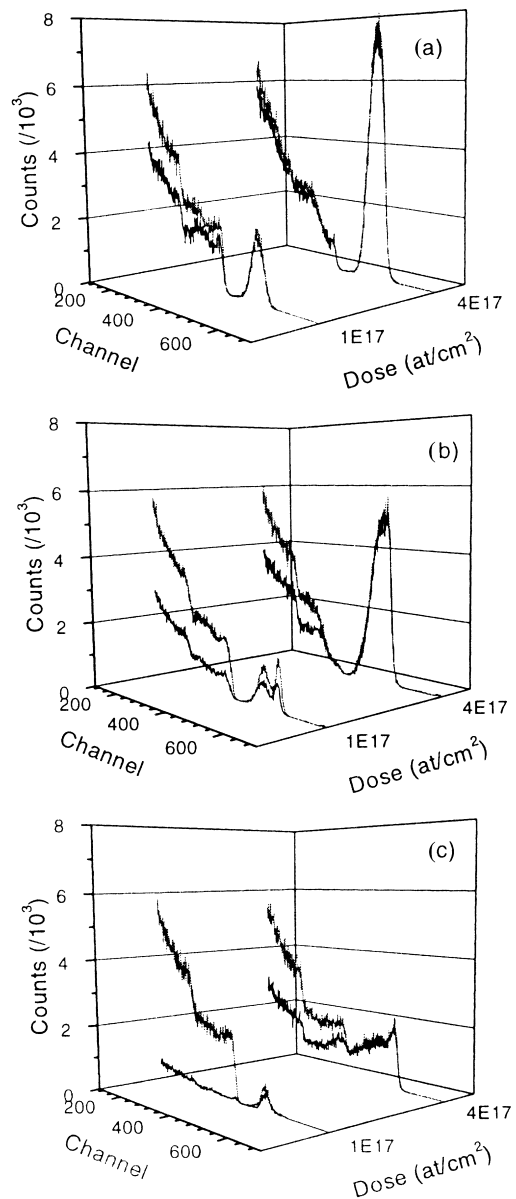


Fig. 4. Aligned and random RBS spectra of *a*-axis-oriented sapphire implanted with $1 \times 10^{17} \text{ Fe}^+/\text{cm}^2$ and $4 \times 10^{17} \text{ Fe}^+/\text{cm}^2$ before (a) and after the annealing in reducing (b) and oxidizing atmosphere (c).

reddish brown. The X-ray diffraction spectrum of the sample annealed in a reducing atmosphere does not reveal the presence of any iron compound.

Fig. 6 shows the magnetization curves measured for the samples implanted with $4 \times 10^{17} \text{ Fe}^+/\text{cm}^2$ before and after different annealings. The curve obtained after implantation shows the formation of a ferromagnetic system. This is due to the high dose of iron present at the surface allowing the creation of an almost continuous nearly metallic layer. The magnetization decreases drastically after the annealing at 1100°C in reducing atmosphere. One explanation for this decrease could be the redistribution of the iron ions in the implanted layer as observed by RBS (Fig. 4c), which was accompanied by the loss of the implanted Fe. The remaining iron is more diluted, dispersed in small precipitates or isolated ions, leading to a decrease of the magnetic component of the magnetization curve. This redistribution and loss of iron, not found in the *c*-cut samples, explains the totally different magnetic properties observed in the two kinds of samples after annealing. The anisotropy in the iron diffusion could be the reason for that. In the samples annealed in oxidizing atmosphere the ferromagnetic component disappears after the first annealing and only the diamagnetic contribution of sapphire was observed.

4. Conclusions

Implantation of high fluences of iron in sapphire leads to the formation of metallic precipitates during the implantation. Above $2 \times 10^{17} \text{ Fe}^+/\text{cm}^2$ a layer with metallic characteristics develops at the surface, leading to a strong ferromagnetic behaviour. The microstruc-

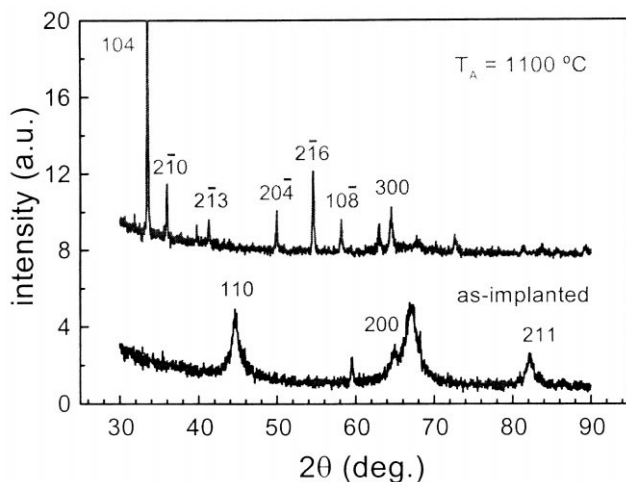


Fig. 5. XRD spectra for *a*-axis-oriented sapphire implanted with $4 \times 10^{17} \text{ Fe}^+/\text{cm}^2$ before and after annealing at 1100°C in an oxidizing atmosphere.

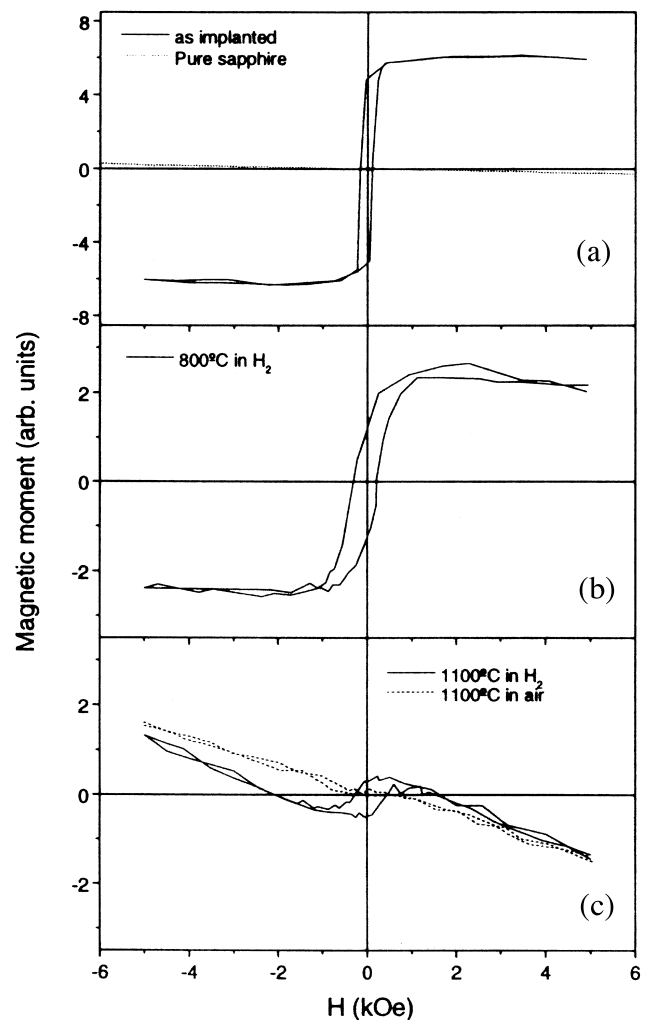


Fig. 6. Magnetization curves for *a*-axis-oriented sapphire after implantation with $4 \times 10^{17} \text{ Fe}^+/\text{cm}^2$ (a) and after annealing at 800°C (b) and 1100°C (c) in a reducing atmosphere. The dashed curve in (c) was obtained for a sample annealed in an oxidizing atmosphere.

tures developed during annealing are strongly dependent on the substrate orientation and annealing atmosphere. For (0001) $\alpha\text{-Al}_2\text{O}_3$ samples annealed in reducing atmosphere we observe the formation of elongated metallic iron precipitates parallel to the surface whose dimension increases with ion fluence. The samples display ferromagnetic behaviour after annealing at 1100°C . The ferromagnetism in the (11 $\bar{2}$ 0) $\alpha\text{-Al}_2\text{O}_3$ samples decreases after similar annealing due to diffusion and loss of iron. Annealing in an oxidizing atmosphere leads to the formation of non-magnetic mixed oxide compounds in the implanted region.

Acknowledgements

This work was partially supported by PRAXIS XXI under contract C/CTM/12067/1998 and the US Department of Energy, Division of Materials Sciences

under contract DE-AC05-96OR22464 with the Lockheed Martin Energy Research Corporation.

References

- [1] T. Miyazaki, N. Tezuka, *J. Magn. Magn. Mater.* 139 (1995) L231.
- [2] C.J. MacHargue, S.X. Ren, P.S. Sklad, L.F. Allard, J. Hunn, *Nucl. Instrum. Methods B* 116 (1996) 173.
- [3] C.J. MacHargue, G.C. Farlow, P.S. Sklad et al., *Nucl. Instrum. Methods B* 19/20 (1987) 813.
- [4] C.J. MacHargue, P.S. Sklad, C.W. White, J.C. McCallum, A. Perez, G. Marest, *J. Mater. Res.* 6 (1991) 2160.
- [5] M. Ohkubo, T. Hioki, J.-i. Kawamoto, *J. Appl. Phys.* 62 (1987) 3069.
- [6] I. Sakamoto, S. Honda, H. Tanoue, N. Hayashi, H. Yamane, *Nucl. Instrum. Methods B* 148 (1999) 1039.
- [7] Joint Committee on Powder Diffraction Standards, *Powder Diffraction File*, ASTM, Philadelphia, PA, 1992.
- [8] S.X. Ren, C.J. MacHargue, L.F. Allard et al., *Mater. Res. Soc. Symp. Proc.* 373 (1995) 305.
- [9] C.J. MacHargue, E. Alves, M.F. da Silva, J.C. Soares, *Nucl. Instrum. Methods B* 148 (1999) 730.